The effect of the phase transition on the optical properties of the lanthanum monopnictide compounds

2008 J. Phys.: Condens. Matter 20 325207

(http://iopscience.iop.org/0953-8984/20/32/325207)

IOP PUBLISHING JOURNAL OF PHYSICS: CONDENSED MATTER

J. Phys.: Condens. Matter **20** (2008) 325207 (12pp) doi:10.1088/0953-8984/20/32/325207

The effect of the phase transition on the optical properties of the lanthanum monopnictide compounds

Ali Hussain Reshak[1], **Z Charifi**[2,3] **and H Baaziz**[2]

[1] Institute of Physical Biology, South Bohemia University, Institute of System Biology and Ecology, Academy of Sciences, Nove Hrady 37333, Czech Republic
[2] Physics Department, Faculty of Science and Engineering, University of M'sila, 28000 M'sila, Algeria

E-mail: charifi_z@yahoo.fr

Received 18 January 2008, in final form 17 June 2008
Published 9 July 2008
Online at stacks.iop.org/JPhysCM/20/325207

Abstract

We report results of the optical properties for LaP and LaAs compounds in three phases: rocksalt (B1), CsCl-type (B2) and primitive tetragonal (PT) using the full potential linearized augmented plane wave (FP-LAPW). The local-density approximation (LDA) and the Engel–Vosko-generalized gradient approximation (EV-GGA) were used. We notice that below 19 and 17 GPa respectively, LaP and LaAs maintain the rocksalt structure (B1). Then at high pressure a crystallographic phase transition occurs. The high pressure stabler phase is the tetragonal structure.

We found that using EV-GGA for the B1 phase led to both compounds being semiconductors with an indirect band gap. While for the same phase (B1) the LDA leads to closure of the gap at the Fermi energy making the both compounds metallic in agreement with the previous calculation. For the PT and B2 phases both LDA and EV-GGA show these compounds as metallic. We study the effect of the high pressure and using different approximations on the optical properties of these compounds. We have calculated the optical conductivity and reflectivity spectra for LaAs compounds and compare it with the available experimental data; reasonable agreement was found.

(Some figures in this article are in colour only in the electronic version)

1. Introduction

The rare earth monopnictides and monochalcogenides are some of the structurally simplest materials. The rare earth pnictides, generally, have low carrier, strongly correlated systems [1], and they show dense Kondo behaviour and heavy fermion states [2, 3]. Lanthanum monopnictide LaX (X = P, As) crystallize in a cubic structure of NaCl-type. These compounds undergo a crystallographic transition from B1 (NaCl) structure to a tetragonal structure over the B2 structure, which can be viewed as a distorted CsCl structure [4, 5] as illustrated in figure 1.

The La monopnictides LaX with NaCl crystal have recently attracted particular interest as a proper reference material for the understanding of various anomalous physical properties of other rare earth pnictides [6, 7]. Numerous experimental and theoretical works have studied the pressure behaviour of these compounds [4, 5, 8, 9]. Recently, the electronic, elastic, thermodynamical and vibrational properties of LaAs and LaP in the rocksalt phase have been studied by performing *ab initio* calculations within the local-density approximation (LDA) [10]. Up to now, most experimental and theoretical studies have been concentrated on the structural, electronic properties [11] of LaP and LaAs. To the best of our knowledge no experimental data or theoretical calculations for the optical properties of LaP and LaAs compounds at ambient and high pressure have been reported yet, apart from one report by Kimura *et al* [12] in which they measured the optical conductivity and reflectivity for LaAs compound.

[3] Author to whom any correspondence should be addressed.

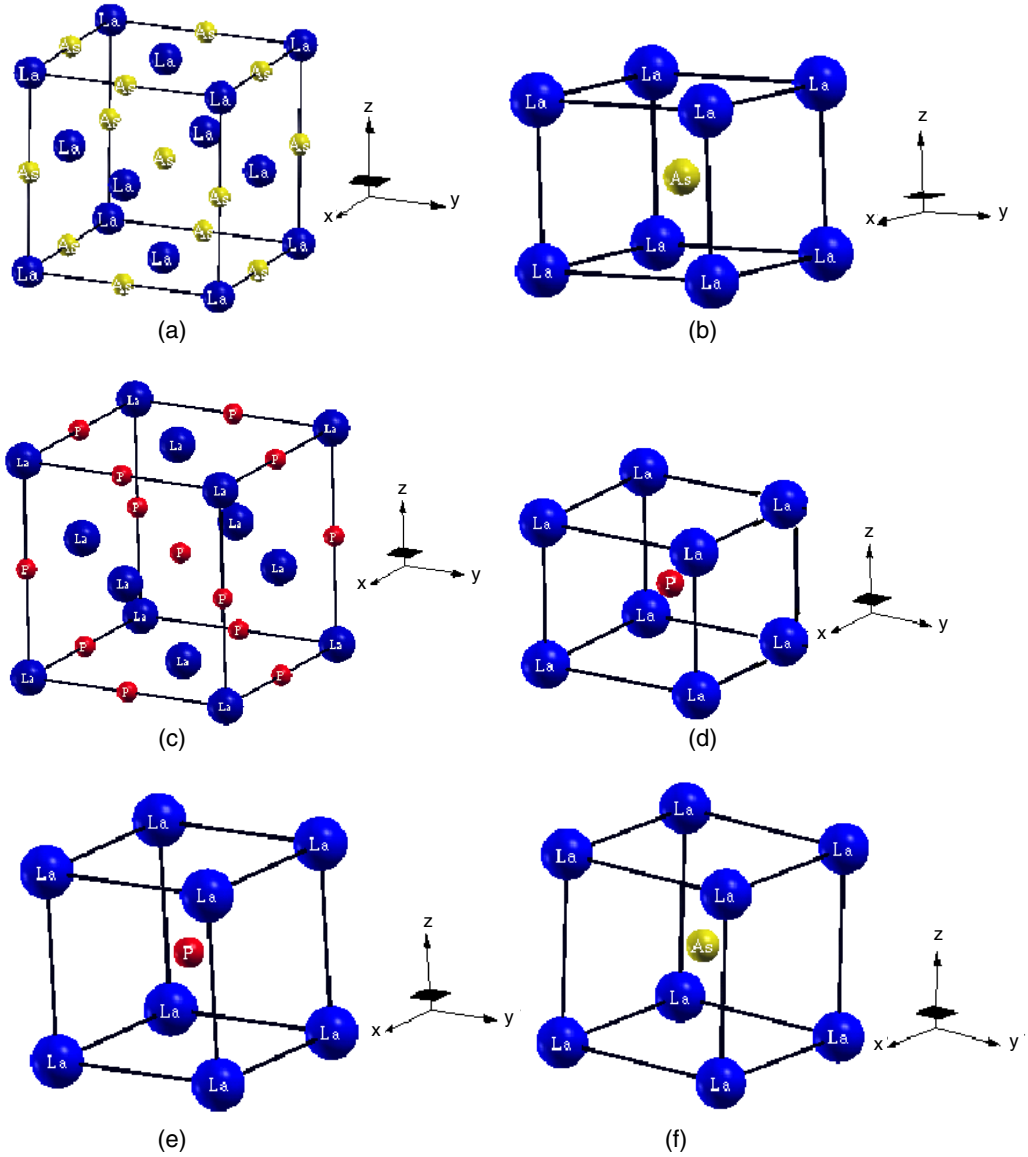

Figure 1. Structure of LaAs and LaP: (a) and (c) B1 phase. (b) and (d) PT phase and (e) and (f) B2 phase.

Measurements and calculations of optical properties have long been a powerful tool in studying the electronic structure of solids. Today, knowledge of the refractive indices and absorption coefficients of solids is especially important in the design and analysis of new devices. The dielectric function $\varepsilon(\omega) = \varepsilon_1(\omega) + i\varepsilon_2(\omega)$ fully describes the optical properties of any homogeneous medium at all photon energies $\hbar w$. We think it would be worthwhile to perform first principles calculations of the optical properties using the state-of-the-art full potential linear augmented plane wave method [13] which has proven to be one of the most accurate methods [14, 15] for the computation of the electronic structure and optical properties of solids within density functional theory (DFT). Hence the effect of the full potential on the electronic structure and the optical properties can be ascertained. High pressure is also a very efficient tool for understanding the electronic structure and hence the optical properties. Our calculations will demonstrate the effect of high pressure and using different approximations on the optical properties of LaP and LaAs compounds.

This paper is organized as follows. In section 2, we give a brief description of the method used and details of the calculations, in section 3, results of the optical properties are presented and analysed. Conclusions are drawn in the last section (section 4).

2. Details of calculations

The lanthanum monopnictides LaP and LaAs crystallize in the simple rocksalt structure (B1) type with space group symmetry $Fm3m$. The La atom is positioned at (0, 0, 0) and the pnictogen at (0.5, 0.5, 0.5). The structure of the high pressure phase of LaP and LaAs is tetragonal which can be viewed as a distorted CsCl structure [5] with La at (0, 0, 0) and the pnictogen at (0.5, 0.5, 0.5) with space group symmetry $P4/mmm$. The PT phase is more stable than the B2 phase at high pressure. The B2 phase

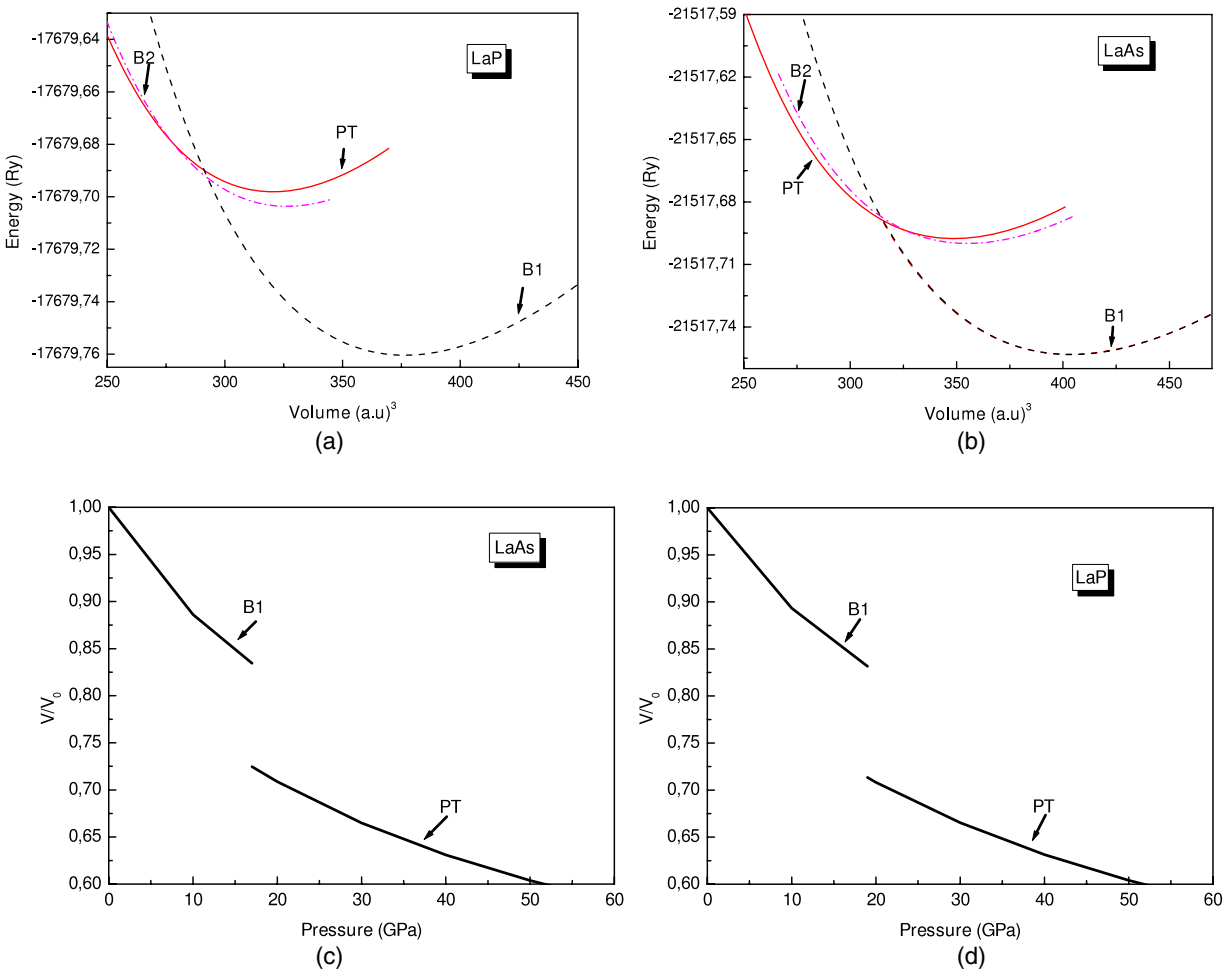

Figure 2. Variation of total energies as a function of volume of unit cell for B1 phase (dashed curve), PT phase (solid curve) and B2 phase (dot–dashed curve) using GGA for: (a) LaP compound, (b) LaAs compound, (c) and (d) diagram showing how the transition pressure is calculated for both compounds.

is a CsCl structure with La at (0, 0, 0) and the pnictogen at (0.5, 0.5, 0.5) with space group symmetry $Pm3m$.

We have performed calculations using the full potential linearized augmented plane wave (FP-LAPW) method as incorporated in the WIEN2K code [13]. This is an implementation of the density functional theory (DFT) with different possible approximations for exchange correlation (XC) potentials. The exchange correlation potential was calculated using both the local-density approximation (LDA) [16] and the generalized gradient approximation (GGA) in the form proposed by Perdew *et al* [17] which is based on exchange–correlation energy optimization to calculate the total energy. Also we have used the Engel–Vosko (EV-GGA) formalism [18], which optimizes the corresponding potential for band structure calculations. It is well known in the self-consistent band structure calculation within DFT, both LDA and GGA usually underestimate the energy gap [19]. This is mainly due to the fact that they have simple forms that are not sufficiently flexible to accurately reproduce both exchange–correlation energy and its charge derivative. Engel and Vosko considered this shortcoming and constructed a new functional form of GGA [18] which is able to better reproduce the exchange potential at the expense of less agreement in the exchange energy. This approach called EV-GGA, yields better band splitting and some other properties which mainly depend on the accuracy of exchange correlation potential. On the other hand the quantities which depend on an accurate description of E_x, such as the equilibrium volume and bulk modulus are in poor agreement with experiment [18], where the structural properties the exchange correlation potential were calculated using the GGA [17] and LDA [16]. For optical properties we applied the LDA and EV-GGA scheme [18].

Kohn–Sham wavefunctions were expanded in terms of spherical harmonics inside non-overlapping muffin-tin (MT) spheres surrounding the atomic sites and as Fourier series in the interstitial region. Inside the muffin-tin spheres, the l expansion of the non-spherical potential and charge density were carried out up to $l_{\max} = 10$.

We have calculated the total energy at several volumes around the equilibrium (see figures 2(a) and (b)). The results are fitted to the Murnaghan's equation of states [20]. In this way we obtained the equilibrium lattice constant. The calculated lattice constants were used to optimize the c/a ratio of the tetragonal cell with constant volume. Figure 2 shows the stability of the PT phase at high pressure, and the B1 phase at ambient pressure. B2 is an unstable phase, so only the

Table 1. Calculated lattice parameters using LDA and GGA, in comparison with the available previous calculations and the experimental data for LaP and LaAs compounds in three phases.

	LaP				LaAs			
B1	Present LDA	Present GGA	Exp.	Others	Present LDA	Present GGA	Exp.	Others
Lattice parameter (Å)	$a = 5.9446$	$a = 6.0628$	6.013 [29] 6.025 [4]	5.851 [3]	$a = 6.0718$	$a = 6.2058$	6.125 [29] 6.137 [4]	5.997 [8]
PT	Present LDA	Present GGA	Exp.	Others	Present LDA	Present GGA	Exp.	Others
Lattice parameter (Å)	$a = 3.711$ $c = 3.82$ $c/a = 1.029$	$a = 3.79$ $c = 3.88$ $c/a = 1.023$	3.461(6) [5] 3.008(8) [5] 0.87 [5]	3.53 [8] 3.059 [8] 0.87 [8]	$a = 3.82$ $c = 3.29$ $c/a = 0.861$	$a = 3.9161$ $c = 3.4062$ $c/a = 0.8698$	3.625(4) [4] 3.06 [4] 0.844 [4]	3.645(6) [8] 3.171 [8] 0.86 [8]
B2	Present LDA	Present GGA	Exp	Others	Present LDA	Present GGA	Exp.	Others
Lattice parameter (Å)	$a = 3.567$	$a = 3.643$			$a = 3.6576$	$a = 3.747$		

transition from B1 to PT is possible for these two compounds.

The corresponding equilibrium lattice parameter, c/a obtained within the LDA and GGA are summarized and compared with experimental and theoretical data in table 1. In order to achieve energy eigenvalue convergence, the wavefunctions in the interstitial region were expanded in plane waves with a cut-off of $K_{\max} = 9/R_{\mathrm{MT}}$ where R_{MT} is the radius of the smallest muffin-tin sphere. Self-consistency was obtained using 56 special k points in the irreducible wedge of the irreducible Brillouin zone (IBZ) for the B1 and B2 phase, and 126, 147 for the PT phases of LaP and LaAs compounds respectively. For the calculation of the optical properties, a dense mesh of uniformly distributed k points is required. Hence, the Brillouin zone integration was performed using the tetrahedron method [21, 22] with 220 in the IBZ for the B1 and B2 phases, 450 and 495 in the IBZ for the PT phases of LaP and LaAs respectively.

LaP and LaAs compounds turn from the initial structure B1 to the PT structure under pressure. The stability of a particular structure is decided by the minima of the Gibbs energy given by [23]:

$$G = E_{\mathrm{tot}} + PV - TS.$$

Since the theoretical calculations are performed at 0 K the free energy becomes equal to the enthalpy (H):

$$H = E_{\mathrm{tot}} + PV.$$

At a given pressure a stable structure is one for which enthalpy has its lowest value and the transition pressure is calculated at which the enthalpies for the two phases are equal. Pressure induced transitions occur at the compressions corresponding to the slope of the common tangents (see figures 2(a)–(d)). The B1 phase is stable at ambient conditions, and the PT phase is more stable than the B2 phase at high pressure.

3. Results and discussion

Optical properties

The dielectric function $\varepsilon(\omega) = \varepsilon_1(\omega) + \mathrm{i}\varepsilon_2(\omega)$ fully describes the optical properties of any homogeneous medium at all photon energies. At the ambient pressure LaP and LaAs compounds crystallized in a cubic structure of NaCl-type (B1). For calculating the optical properties of cubic structural material we need only one dielectric tensor component to completely characterize the linear optical properties. This component is $\varepsilon_2(\omega)$ the imaginary part of the frequency dependent dielectric function given by [24]

$$\varepsilon_2(\omega) = \frac{8}{3\pi\omega^2} \sum_{nn'} \int_{\mathrm{BZ}} |P_{nn'}(k)|^2 \frac{\mathrm{d}S_k}{\nabla\omega_{nn'}(k)},$$

where $P_{nn'}(k)$ is the dipolar matrix elements between initial $|nk\rangle$ and final $|n'k\rangle$ states with the eigenvalues $E_n(k)$ and $E_{n'}(k)$, respectively.

At the high pressure, above 19 and 17 GPa respectively, both LaAs and LaP compounds transform from the NaCl-type structure to the tetragonal structure (PT) [4, 5]. The tetragonal symmetry has many components in the dielectric tensor. In this calculation we will concentrate on the major components, corresponding to electric vector $\vec{E}$ parallel or perpendicular to the c axis. The corresponding dielectric functions are $\varepsilon^{\parallel}(\omega)$ and $\varepsilon^{\perp}(\omega)$. The calculations of these dielectric functions involve the energy eigenvalues and electron wavefunctions. These are the natural outputs of band structure calculations. We have performed calculations of the imaginary part of the interband frequency dependent dielectric function using the expressions [25]

$$\varepsilon_2^{\parallel}(\omega) = \frac{12}{m\omega^2} \int_{\mathrm{BZ}} \sum_{nn'} \frac{|P^Z_{nn'}(k)|^2 \,\mathrm{d}S_k}{\nabla\omega_{nn'}(k)}$$

$$\varepsilon_2^{\perp}(\omega) = \frac{6}{m\omega^2} \int_{\mathrm{BZ}} \sum_{nn'} \frac{\left[|P^X_{nn'}(k)|^2 + |P^Y_{nn'}(k)|^2\right] \mathrm{d}S_k}{\nabla\omega_{nn'}(k)}.$$

The above expressions are written in atomic units with $e^2 = 1/m = 2$ and $\hbar = 1$. Where $\hbar\omega$ is the photon energy. $P^X_{nn'}(k)$ and $P^Z_{nn'}(k)$ are the X and Z component of the dipolar matrix elements between initial $|nk\rangle$ and final $|n'k\rangle$ states with their eigenvalues $E_n(k)$ and $E_{n'}(k)$, respectively. $\omega_{nn'}(k)$ is the energy difference

$$\omega_{nn'}(k) = E_n(k) - E_{n'}(k)$$

and S_k is a constant energy surface

$S_k = \{k;\omega_{nn'}(k) = \omega\}$. The integral is over the first Brillouin zone.

The optical properties can be described by means of the transverse dielectric function $\varepsilon(\omega)$. For the metallic materials there are two contribution to $\varepsilon(\omega)$, namely intraband and interband transitions. As the investigated compounds are metallic we must include the Drude term (intraband transitions) [26].

$$\varepsilon_2^{\perp}(\omega) = \varepsilon_{2\text{inter}}^{\perp}(\omega) + \varepsilon_{2\text{intra}}^{\perp}(\omega)$$

where

$$\varepsilon_{2\text{intra}}^{\perp}(\omega) = \frac{\omega_{\text{P}}^{\perp}\tau}{\omega(1+\omega^2\tau^2)}$$

where ω_{P} is the anisotropic plasma frequency [27] and τ is the mean free time between collisions.

$$\omega_{\text{P}}^{\perp 2} = \frac{8\pi}{3}\sum_{kn}\vartheta_{kn}^{\perp 2}\delta(\varepsilon_{kn})$$

where ε_{kn} is $E_n(k) - E_{\text{F}}$ and $\vartheta_{kn}^{\perp}$ is the electron velocity (in the basal plane) squared. Similar expressions for the parallel component can be written.

In order to better understand the optical properties we have calculated the band structure using the LDA and EV-GGA for the B1, B2 and PT phases of LaP and LaAs compounds as shown in figure 3. We note that for the B1 phase the EV-GGA leads to an opening up of an energy gap at Fermi energy (E_{F}) making both LaP and LaAs semiconductors. These gaps are indirect band gaps between the valence band maximum (VBM) located at Γ and the conduction band minimum (CBM) located at X. The values of these gaps are about 0.56 eV for LaP and 0.43 eV for LaAs.

It would be worthwhile to attempt to identify the band transitions that are responsible for the spectral structures in $\varepsilon_2(\omega)$, $\varepsilon_2^{\perp}(\omega)$ and $\varepsilon_2^{\parallel}(\omega)$ using our calculated band structure. Figure 3 shows the transitions which are responsible for the spectral structures in $\varepsilon_2(\omega)$, $\varepsilon_2^{\perp}(\omega)$ and $\varepsilon_2^{\parallel}(\omega)$. For simplicity we have labelled the transitions in figure 3, as A, B, and C. The transitions A are responsible for the structures in $\varepsilon_2(\omega)$, $\varepsilon_2^{\perp}(\omega)$ and $\varepsilon_2^{\parallel}(\omega)$ for energies up to 4.0 eV, transitions B are responsible for the structures in the energy range 4.0–8.0 eV and the transitions C are responsible for the structures between 8.0 and 12.0 eV.

Figure 4 shows the calculated $\varepsilon_2(\omega)$ for the B1 phase of LaP and LaAs compounds using the EV-GGA. We notice that both compounds have a similar optical spectrum that is attributed to the fact that the band structures for these compounds are similar with only minor differences. These minor differences cause some changes in the optical transitions resulting in small changes in the peak positions and the peak heights.

It is known that peaks in the optical response are determined by the electric–dipole transitions between the valence and conduction bands. These peaks can be identified from the band structure. In order to identify these peaks we need to look at the optical transition dipole matrix elements. Our analysis of the $\varepsilon_2(\omega)$ curve show that the first critical points of the dielectric function occur at about 0.7 eV and 0.75 for LaAs and LaP compounds respectively. These points are X_{v}–X_{c} splitting, which gives the thresholds for the optical transition between the VBM and the first CBM for the B1 phase. This is known as the fundamental absorption edge, $\varepsilon_2(\omega)$, and shows pronounced peaks around 3.6 and 3.2 eV for LaP and LaAs respectively.

Figures 5–9 show the calculated $\varepsilon_2(\omega)$, $\varepsilon_2^{\parallel}(\omega)$ and $\varepsilon_2^{\perp}(\omega)$ for the B1, B2 and PT phases of LaP and LaAs compounds using the LDA and EV-GGA. We note that for the B1 phase the LDA leads to a closure of the gap at the Fermi energy making both compounds metallic in agreement with the previous band structure calculations [11]. For the B2 and PT phases both the LDA and EV-GGA show these compounds as metallic. We have performed calculations of $\varepsilon_2(\omega)$, $\varepsilon_2^{\parallel}(\omega)$ and $\varepsilon_2^{\perp}(\omega)$ with and without the Drude term. The effect of the Drude term is significant for energies less than 1 eV. The sharp rise at low energies is due to the Drude term. We note that there is a considerable anisotropy between $\varepsilon_2^{\parallel}(\omega)$ and $\varepsilon_2^{\perp}(\omega)$ for both the LDA and EV-GGA. All the structures are shifted towards lower energies. The shifting of the structures is consistent with our calculated band structure and density of states. In the low energy range $\varepsilon_2^{\parallel}(\omega)$ dominates. Thereafter, both polarizations contribute.

If we compare figures 4 and 6 for both compounds under the B1 phase using different approximations (LDA and EV-GGA) we notice that the optical spectra for both approximations are similar expect that the LDA underestimates the energy band gap resulting in a closed energy gap characteristic of metallic behaviour. That is the reason we see the sharp rise in the optical spectra of both compounds (figure 6). If we compare figure 5 with figure 7, for both compounds under the PT phase we find the optical spectra of both compounds using the LDA shows more structure in the low energy range. That is attributed to the fact that the LDA underestimates the energy gap resulting in a shift of both VBM and CBM towards E_{F} causing more bands to cut E_{F} than in the case of the EV-GGA.

In order to investigate the effect of high pressure on the optical properties we need to compare figure 4 with figure 5 and figure 6 with figure 7. We find that under high pressure (PT phase) both compounds became metallic (figure 5) in comparison with figure 4 using the same approximation (EV-GGA). In figure 7, the LDA under high pressure shows a very high pronounced sharp rise at low energies in comparison to figure 6. In general, all the structures in the PT phase are shifted towards lower energies by around 2 eV with significant increases in the peak heights in comparison with the structures in the B1 phase.

Generally the peaks in the optical response are determined by the electric–dipole transitions between the occupied and unoccupied bands. We analysed the optical spectra of $\varepsilon_2(\omega)$, $\varepsilon_2^{\parallel}(\omega)$ and $\varepsilon_2^{\perp}(\omega)$ and found that the transitions which are responsible for the structures below 5 eV in $\varepsilon_2(\omega)$, $\varepsilon_2^{\parallel}(\omega)$ and $\varepsilon_2^{\perp}(\omega)$ are dominated by transitions from bands just below the Fermi energy (E_{F}) to bands just above it. In contrast the transitions which are responsible for the structures above 5 eV in $\varepsilon_2(\omega)$, $\varepsilon_2^{\parallel}(\omega)$ and $\varepsilon_2^{\perp}(\omega)$ are dominated by transitions from top (and bottom) of the As/P-s states to the La-d states.

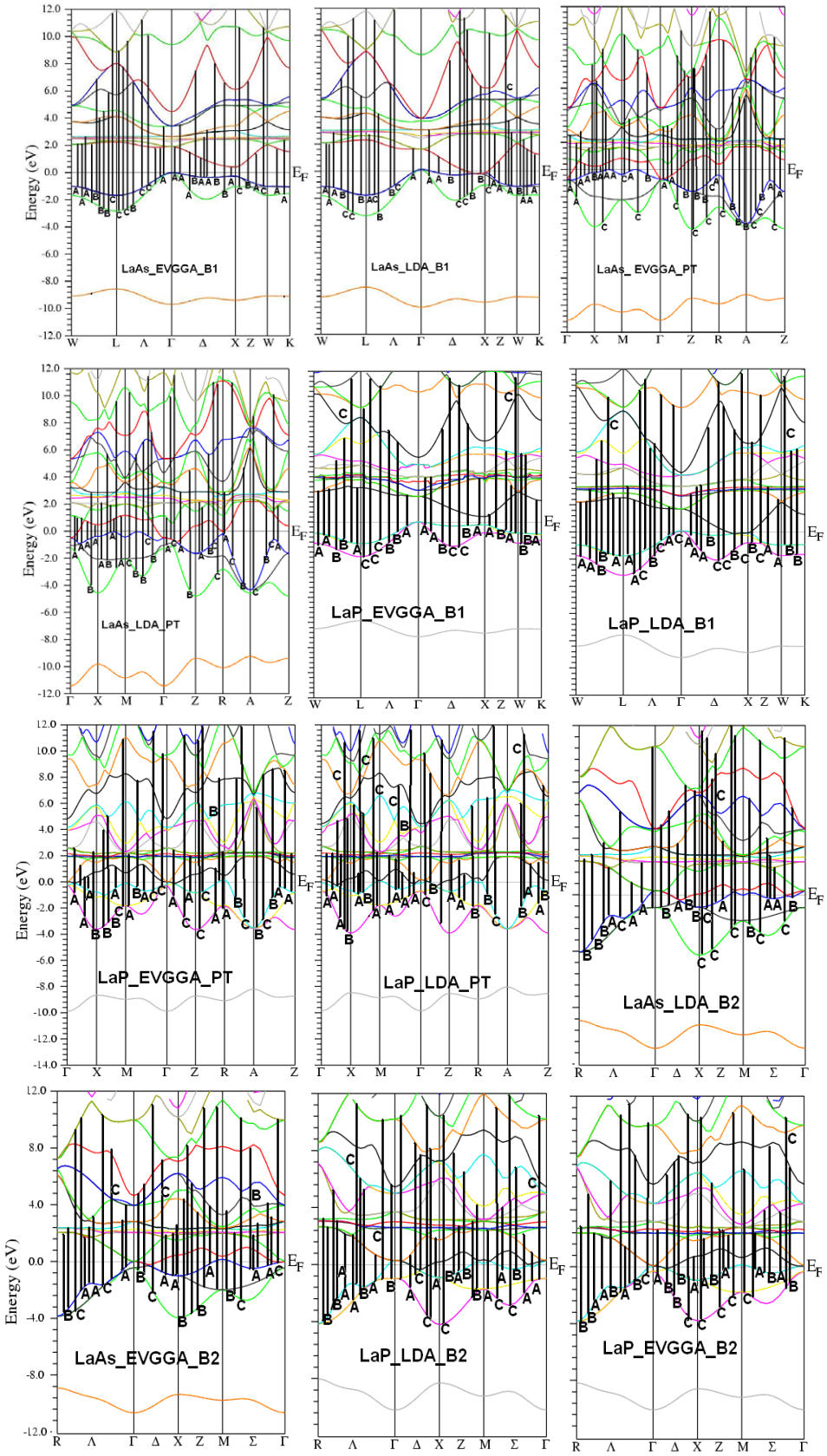

Figure 3. Calculated band structure for the B1 and PT and B2 phases of LaP and LaAs compounds using the LDA and EV-GGA.

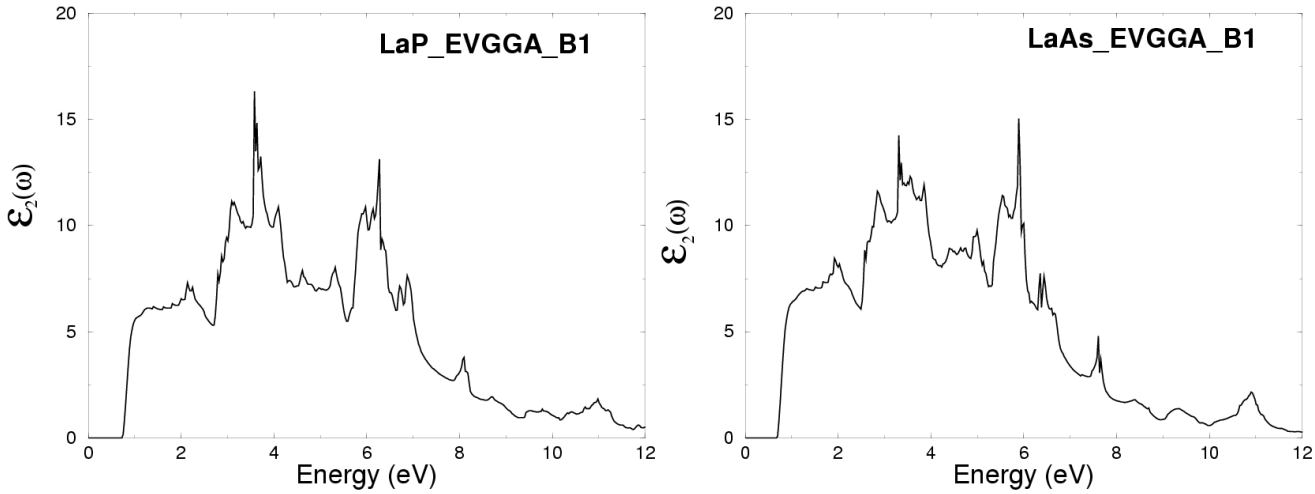

Figure 4. Calculated $\varepsilon_2(\omega)$ for the B1 phase of LaP and LaAs compounds using the EV-GGA.

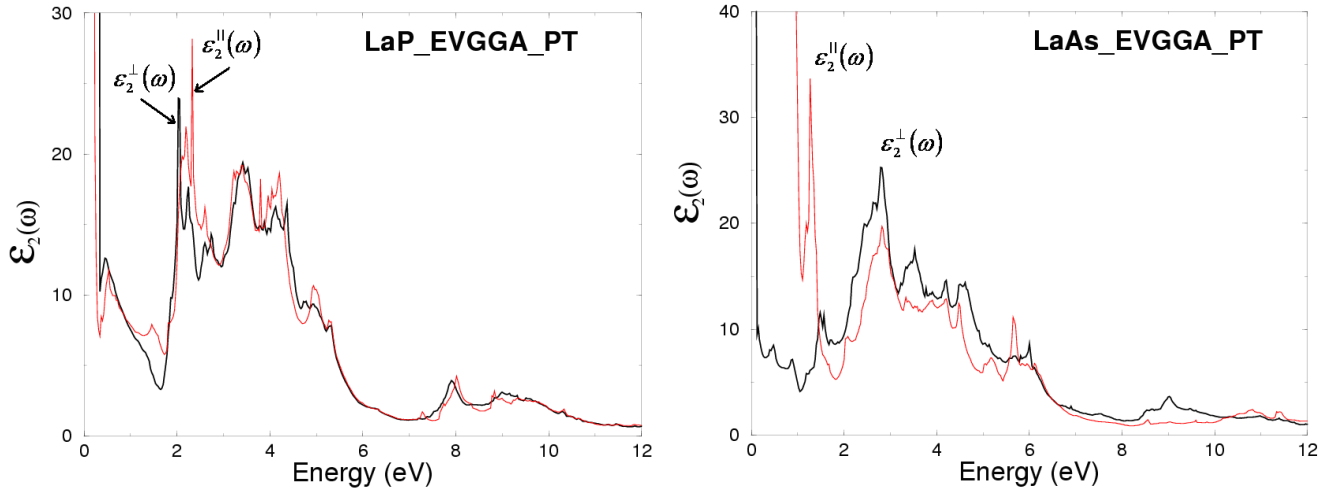

Figure 5. Calculated $\varepsilon_2^{\perp}(\omega)$ (dark curve) and $\varepsilon_2^{\parallel}(\omega)$ (light curve) for the PT phase of LaP and LaAs compounds using the EV-GGA.

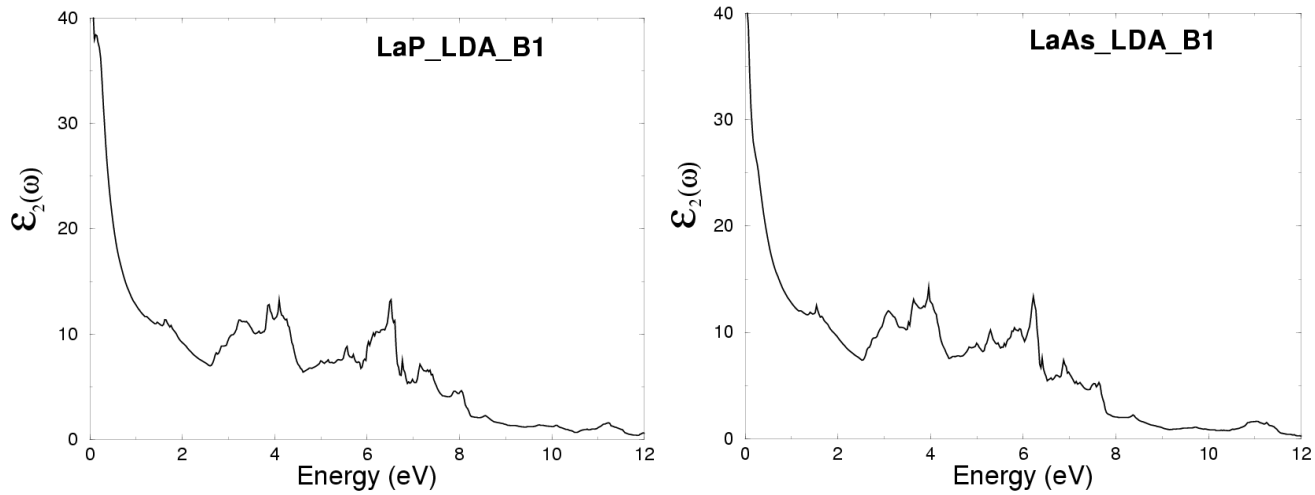

Figure 6. Calculated $\varepsilon_2(\omega)$ for the B1 phase of LaP and LaAs compounds using the LDA.

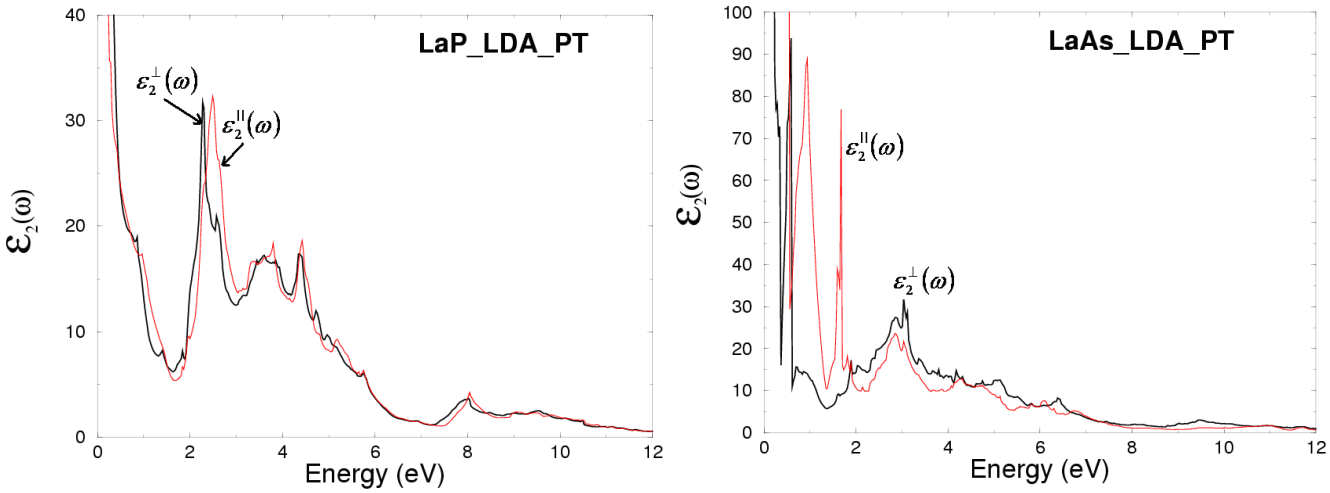

Figure 7. Calculated $\varepsilon_2^{\perp}(\omega)$ (dark curve) and $\varepsilon_2^{\parallel}(\omega)$ (light curve) for the PT phase of LaP and LaAs compounds using the LDA.

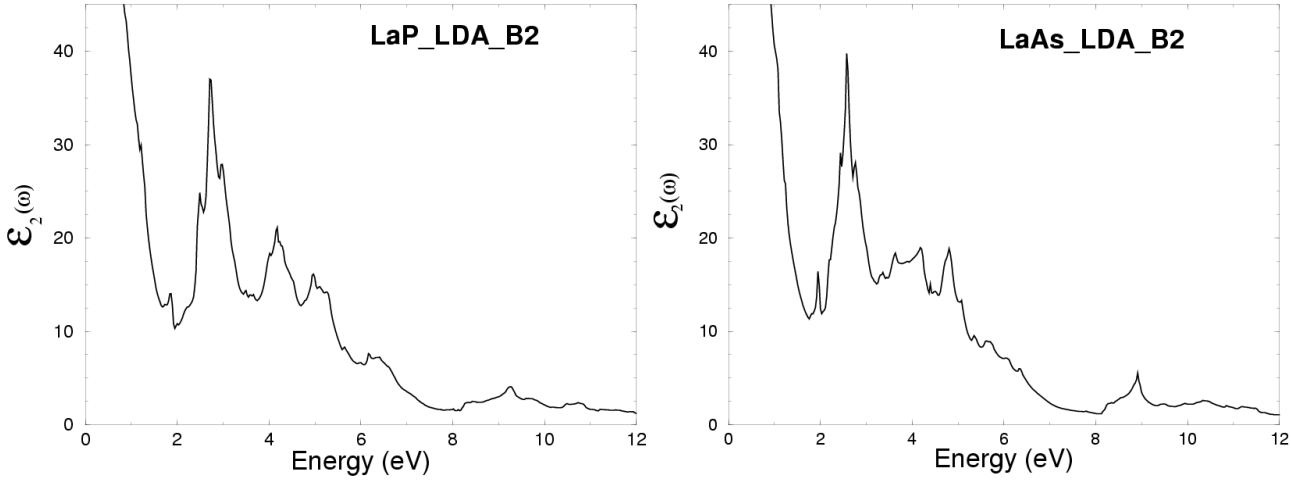

Figure 8. Calculated $\varepsilon_2(\omega)$ for the B2 phase of LaP and LaAs compounds using the LDA.

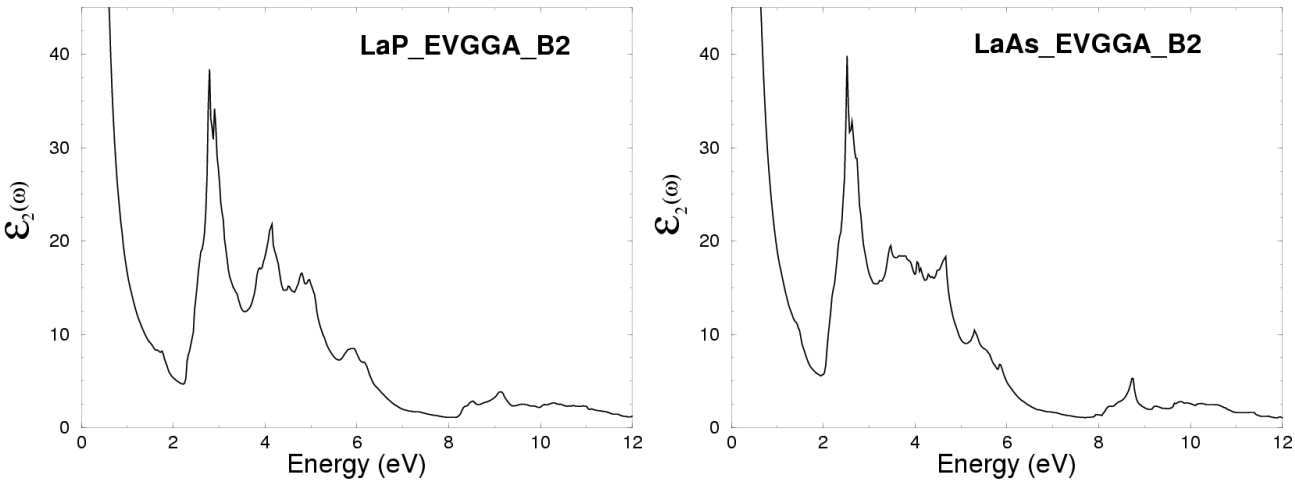

Figure 9. Calculated $\varepsilon_2(\omega)$ for the B2 phase of LaP and LaAs compounds using the EV-GGA.

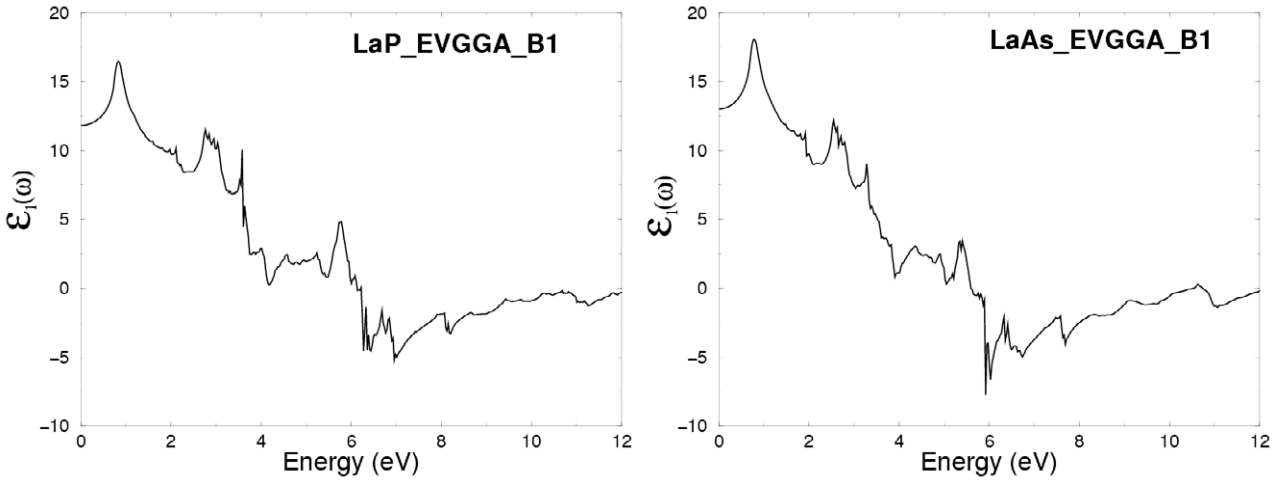

Figure 10. Calculated $\varepsilon_1(\omega)$ for B1 phase of LaP and LaAs compounds using EV-GGA.

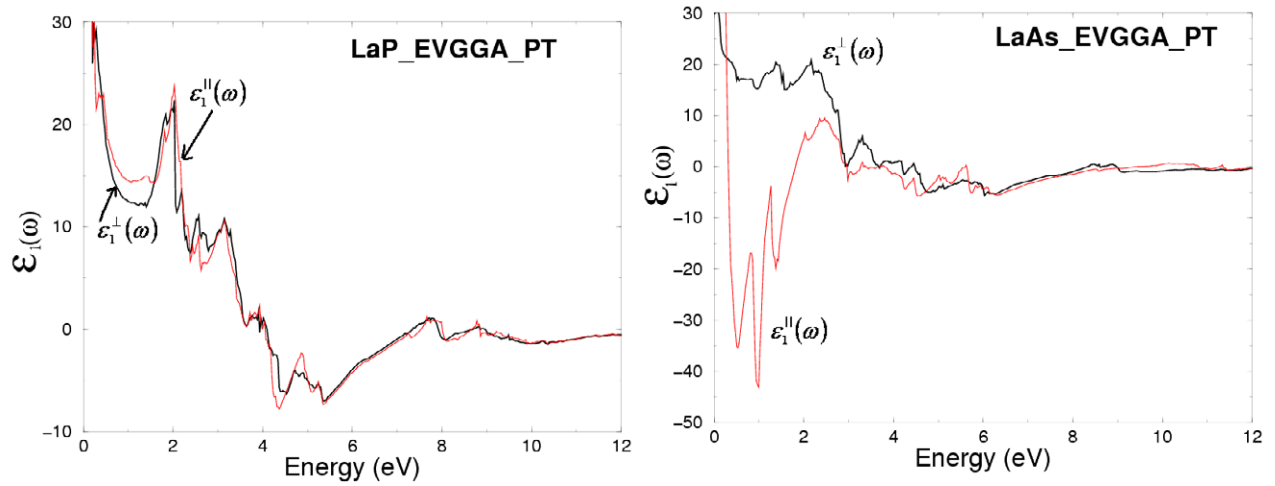

Figure 11. Calculated $\varepsilon_1^{\perp}(\omega)$ (dark curve) and $\varepsilon_1^{\parallel}(\omega)$ (light curve) for PT phase of LaP and LaAs compounds using EV-GGA.

The real parts $\varepsilon_1(\omega)$, $\varepsilon_1^{\parallel}(\omega)$ and $\varepsilon_1^{\perp}(\omega)$ are obtained using the Kramers–Kronig relations [26].

$$\varepsilon_1(\omega) = 1 + \frac{2}{\pi} P \int_0^{\infty} \frac{\omega' \varepsilon_2(\omega')}{\omega'^2 - \omega^2} \, \mathrm{d}\omega'$$

where P implies the principal value of the integral.

Figure 10 shows $\varepsilon_1(\omega)$ for B1 phase of LaP and LaAs compounds using EV-GGA. Again we notice that the optical spectra are similar. The first structure around 1 eV shows the highest peak intensity in these spectra. The main peak is followed by small structures oscillating around the zero position, then goes to negative values at high energies. The calculated $\varepsilon_1(0)$ are 12.0 and 13.0 for LaP and LaAs respectively. We note that a smaller energy gap yields a larger $\varepsilon_1(0)$ value. This could be explained on the basis of the Penn model [28]. The Penn model is based on the expression $\varepsilon(0) \approx 1 + (\hbar\omega_{\mathrm{P}}/E_{\mathrm{g}})^2$. It is clear that $\varepsilon(0)$ is inversely proportional to E_{g}. Hence, a smaller E_{g} yields a larger $\varepsilon(0)$. We can determine E_{g} from this expression by using the values of $\varepsilon(0)$ and the plasma energy $\hbar\omega_{\mathrm{P}}$.

Figures 11–15 show $\varepsilon_1(\omega)$, $\varepsilon_1^{\parallel}(\omega)$ and $\varepsilon_1^{\perp}(\omega)$ for the B1, B2 and PT phases of LaP and LaAs compounds using LDA and EV-GGA approximations. In the low energy range the effect of Drude term is considerable. The calculated $\varepsilon_1^{\parallel}(\omega)$ and $\varepsilon_1^{\perp}(\omega)$ is anisotropic. In the low energy range up to 3 eV, $\varepsilon_1^{\parallel}(\omega)$ dominates, thereafter both polarizations contribute.

In order to make detailed comparison with the experimental data, we have calculated the optical conductivity (OC) spectra for the B1 phase of LaAs compounds and compared it with the available experimental data. The optical conductivity $\sigma(\omega)$ is related to the dielectric function $\varepsilon(\omega)$ as $\varepsilon(\omega) = 1 + \frac{4\pi i\sigma(\omega)}{\omega}$. The calculated OC along with experimental data are shown in figure 16. There is a reasonable agreement between calculation and experiment [12] for a number of the spectral features, which are interpreted by specific interband transitions within the calculated band structure. We tried various values of the broadening to simulate the experimental broadening due to finite life-time; small values give a peaky spectrum while large values flatten the peaks, weakening the structure. The results presented here are for zero broadening. The peaks in the opti-

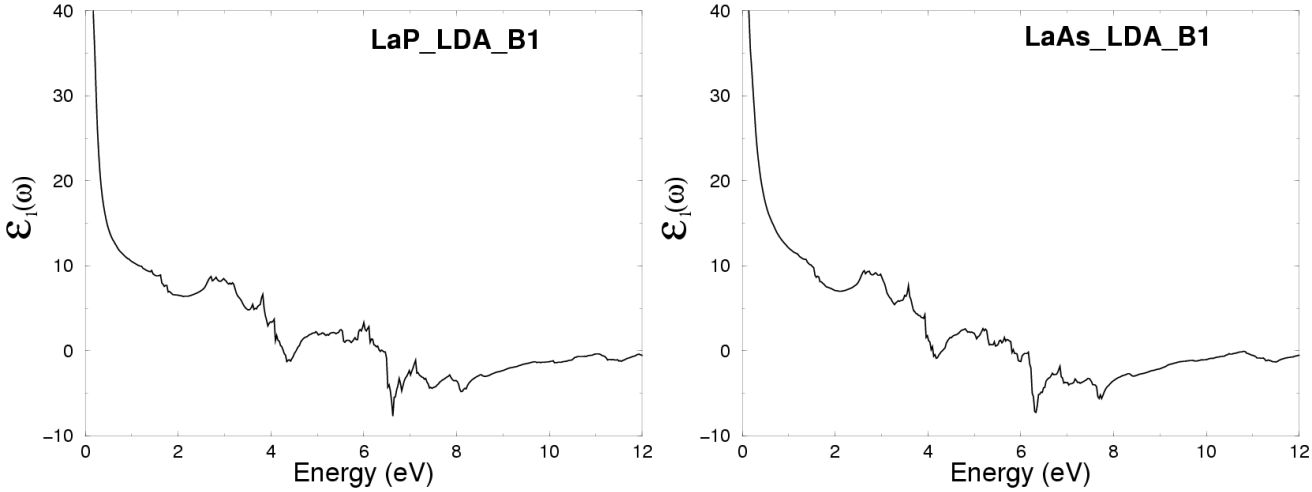

Figure 12. Calculated $\varepsilon_1(\omega)$ for B1 phase of LaP and LaAs compounds using LDA.

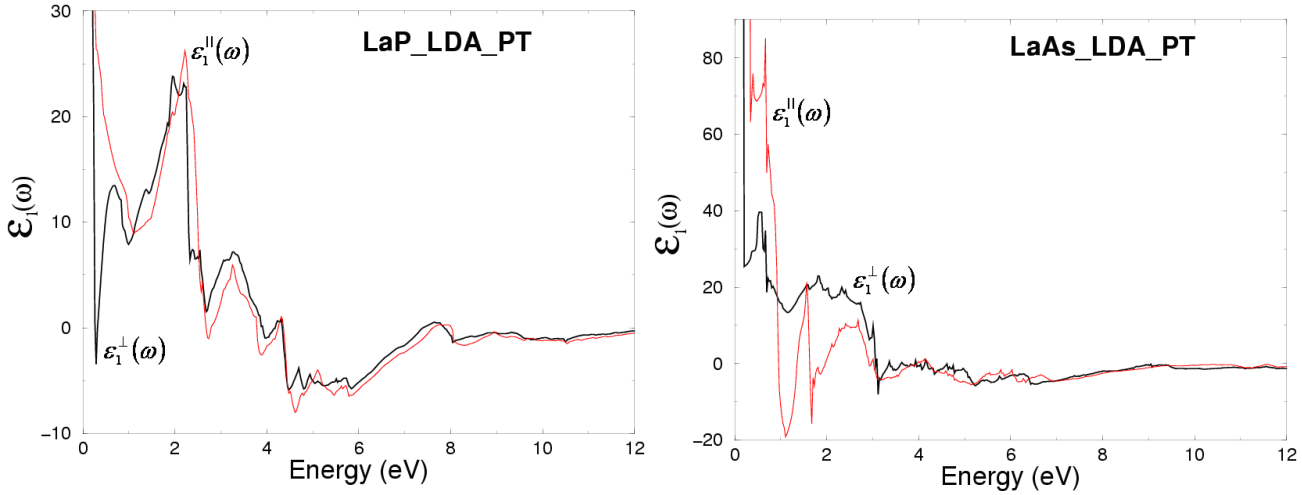

Figure 13. Calculated $\varepsilon_1^{\perp}(\omega)$ (dark curve) and $\varepsilon_1^{\parallel}(\omega)$ (light curve) for PT phase of LaP and LaAs compounds using LDA.

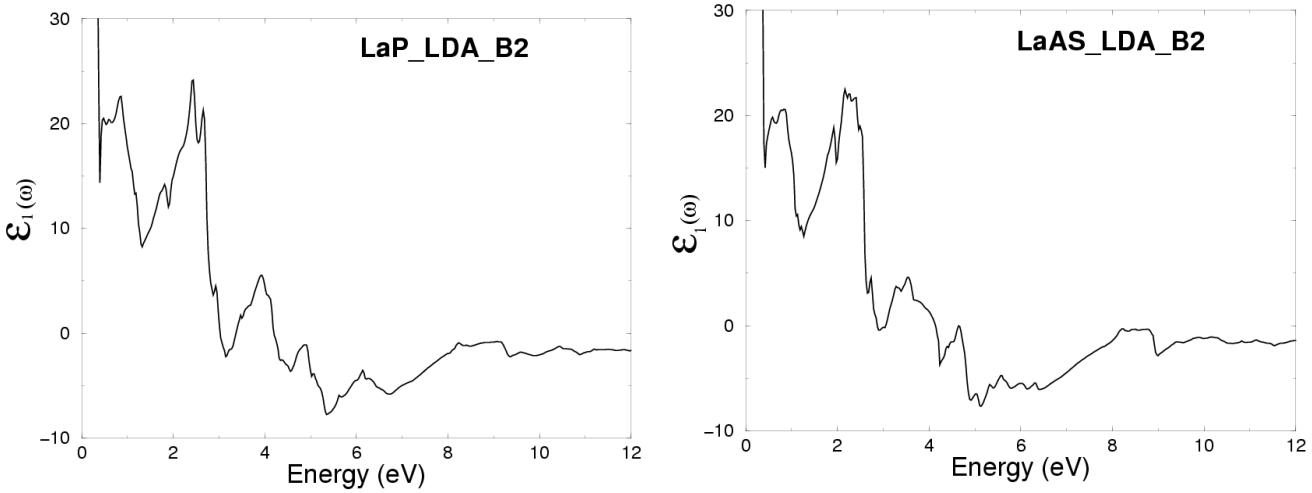

Figure 14. Calculated $\varepsilon_1(\omega)$ for B2 phase of LaP and LaAs compounds using LDA.

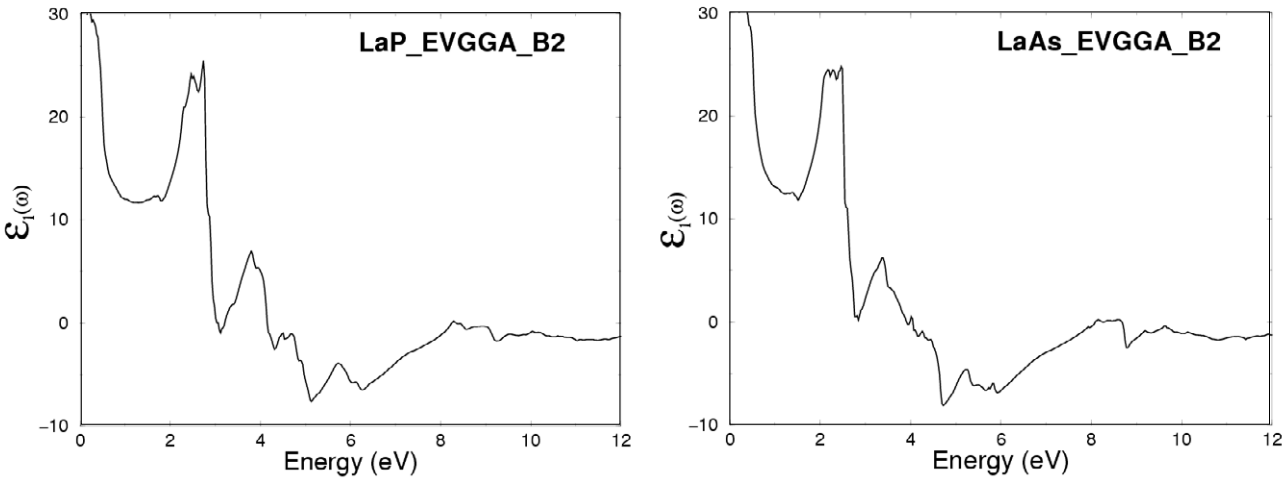

Figure 15. Calculated $\varepsilon_1(\omega)$ for B2 phase of LaP and LaAs compounds using EV-GGA.

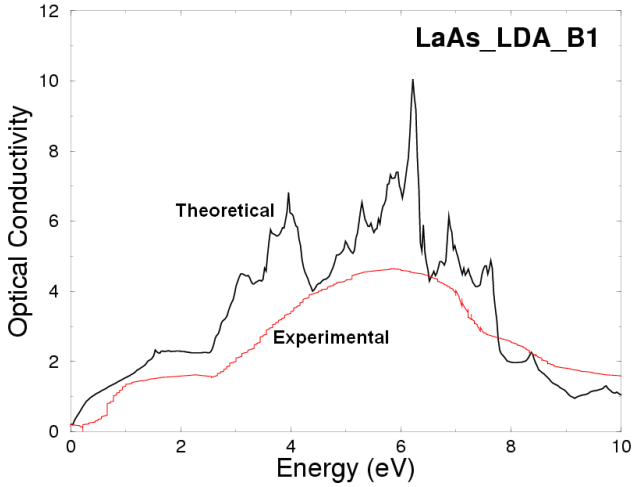

Figure 16. Calculated optical conductivity (dark curve) for B1 phase of LaAs, along with the experimental data (light curve) [12].

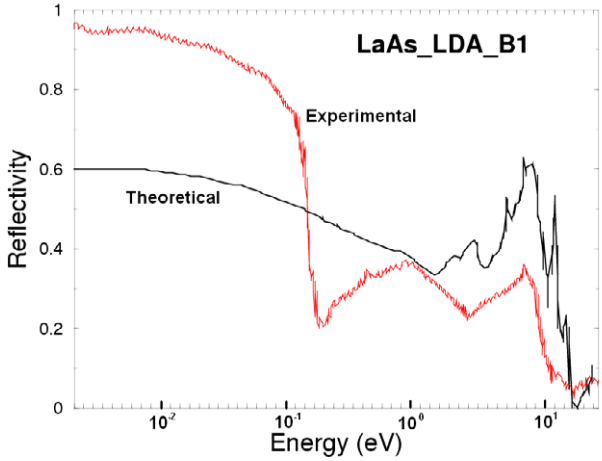

Figure 17. Calculated reflectivity (dark curve) for B1 phase of LaAs, along with the experimental data (light curve) [12], in the photon energy range up to 30 eV in a logarithmic scale.

cal conductivity spectra are determined by the electric–dipole transitions between As-p states (occupied states) to La-d states (unoccupied states).

The knowledge of both the real and imaginary parts of the dielectric function allows the calculation of important optical functions such as the reflectivity [26]

$$R(\omega) = \frac{n + ik - 1}{n + ik + 1}.$$

We have calculated the reflectivity spectra for the B1 phase of the LaAs compound. The reflectivity spectra along with the experimental data [12] are shown in figure 17, in the photon energy range up to 30 eV on a logarithmic scale. We note that in the high energy range our calculated reflectivity is in reasonable agreement with the experimental data. While in the low energy range the first minimum and the first peak need to be shifted towards lower energies to match the experimental data. This reasonable agreement is attributed to our use of the full potential method which has proven to be one of the most accurate methods [14, 15] for the computation of the electronic structure of solids within density functional theory (DFT).

4. Conclusion

We have presented the optical properties of the binary compounds LaP and LaAs for the B1, B2 and PT phases using the FP-LAPW method. In these calculations we used LDA and EV-GGA formalism, which optimizes the corresponding potential for band structure calculations. Below 19 and 17 GPa respectively, LaP and LaAs maintain the rocksalt structure (B1). There then occurs a crystallographic phase transition. For both compounds the high pressure phase is the tetragonal structure. By using the LDA our calculations show that LaP and LaAs are metallic compounds for the two phases B1 and PT in agreement with previous calculations. However using the EV-GGA the two compounds LaP and LaAs in the B1 phase

leads to an opening up of an energy gap at E_F. These gaps are an indirect band gap between the VBM-Γ and CBM-X. The values of these gaps are about 0.56 eV for LaP and 0.43 eV for LaAs. The two compounds remains metallic for the PT phase. In order to make detailed comparisons with the experimental data, we have calculated the optical conductivity (OC) and reflectivity spectra for LaAs compounds and compared it with the available experimental data. Reasonable agreement was found that is attributed to our use of the full potential method which has proven to be one of the most accurate methods for the computation of the electronic structure of solids within density functional theory.

Acknowledgments

This work was supported from the institutional research concept of the Institute of Physical Biology, UFB (No. MSM6007 665808), and the Institute of System Biology and Ecology, ASCR (No. AVOZ60870520).

References

[1] Li D X, Haga Y, Shida H, Suzuki T and Kwon Y S 1996 *Phys. Rev.* B **54** 10483
[2] Yoshida M, Koyama K, Sakon T, Ochiai A and Motokawa M 2000 *J. Phys. Soc. Japan* **69** 3629
[3] Suzuki T 1993 *Physica* B **347** 186
[4] Shirotani I, Yamanashi K, Hayashi J, Ishimatsu N, Shimomura O and Kckegawa T 2003 *Solid State Commun.* **127** 573
[5] Adachi T, Shirotani I, Hayashi J and Shimomura O 1998 *Phys. Lett.* A **250** 389
[6] Hullinger F 1978 *J. Magn. Magn. Mater.* **8** 83
[7] Heer H, Furrer A, Halg W and Vogt O 1977 *J. Phys. C: Solid State Phys.* **12** 5207
[8] Vaitheeswaran G, Kanchana V and Rajagopalan M 2002 *J. Alloys Compounds* **336** 46
[9] Pagare G, Samkar P, Samyal P and Jha K 2005 *J. Alloys Compounds* **398** 16
[10] Deligőy E, Colakoglu K, Ciftci Y O and Ozisik H 2007 *J. Phys.: Condens. Matter* **19** 436204
[11] Hasegawa A 1980 *J. Phys. C: Solid State Phys.* **13** 6147
[12] Kimura S, Arai F, Haga Y, Suzuki T and Kezawa M I 1995 *Physica* B **206** 780
[13] Blaha P, Schwarz K, Madsen G K H, Kvasnicka D and Luitz J 2001 *WIEN2K, An Augmented Plane Wave + Local Orbitals Program for Calculating Crystal Properties* Karlheinz Schwarz, Techn. Universitat, Wien, Austria (ISBN 3-9501031-1-2)
[14] Gao S 2003 *Comput. Phys. Commun.* **153** 190
[15] Schwarz K 2003 *J. Solid State Chem.* **176** 319
[16] Kohn W and Sham L J 1965 *Phys. Rev.* A **140** 1133
[17] Perdew J P, Burke S and Ernzerhof M 1996 *Phys. Rev. Lett.* **77** 3865
[18] Engel E and Vosko S H 1993 *Phys. Rev.* B **47** 13164
[19] Dufek P, Blaha P and Schwarz K 1994 *Phys. Rev.* B **50** 7279
[20] Murnaghan F D 1944 *Proc. Natl Acad. Sci. USA* **30** 244
[21] Jepsen O and Andersen O K 1971 *Solid State Commun.* **9** 1763 Lehmann G and Taut M 1972 *Phys. Status Solidi* B **54** 496
[22] Wilson J A and Yoffe A D 1969 *Adv. Phys.* **18** 193
[23] Born M and Huang K 1954 *Dynanical Theory of Crystal Lattices* (Oxford: Clarendon)
[24] Khan M A, Kashyap A, Solanki A K, Nautiyal T and Auluck S 1993 *Phy. Rev.* B **23** 16974
[25] Hufner S, Claessen R, Reinert F, Straub Th, Strocov V N and Steiner P 1999 *J. Electron Spectrosc. Relat. Phenom.* **100** 191
[26] Wooten F 1972 *Optical Properties of Solids* (New York: Academic)
[27] Chakraborrty B, Pickett W E and Allen P B 1972 *Phys. Rev.* B **14** 3227
[28] Penn D R 1962 *Phys. Rev.* **128** 2093
[29] Wyckoff R W G 1963 *Crystal Structure* 2nd edn, vol 1 (London: Wiley) p 87